Acetylene Cyclotrimerization Catalyzed by TiO_2 and VO_2 in the Gas Phase: A DFT Study

Yan-Ping Ma, Wei Xue, Zhe-Chen Wang, Mao-Fa Ge, and Sheng-Gui He*

Beijing National Laboratory for Molecular Sciences, State Key Laboratory for Structural Chemistry of Unstable and Stable Species, Institute of Chemistry, Chinese Academy of Sciences, Beijing 100080, People's Republic of China

Received: November 20, 2007; In Final Form: February 4, 2008

Density functional theory (DFT) calculations have been used to investigate acetylene cyclotrimerization catalyzed by titanium and vanadium dioxides. The calculated results illustrate that the overall process is highly favorable at room temperature from both thermodynamic and kinetic points of view. The mechanism of C_2H_2 cyclotrimerization over MO_2 (M = Ti, V) can be understood as four steps: (1) a four-membered ring (−O−M−C═C−) formation that coordinates and activates the first C_2H_2 molecule; (2) the second C_2H_2 insertion into the M−C bond to form a six-membered ring (−O−M−C═C−C═C−); (3) the third C_2H_2 insertion into the M−C bond to form an eight-membered ring (−O−M−C═C−C═C−C═C−); and (4) contraction of the eight-membered ring and benzene formation and desorption. All of the reaction steps are overall barrierless with respect to the separated reactants ($MO_2C_{2x}H_{2x} + C_2H_2$, $x = 0, 1, 2$). This theoretical study predicts that the M═O double bond in MO_2 is very catalytic toward the C_2H_2 cyclotrimerization. The metal center in this study can be considered always in the same +4 oxidation state (Ti^{4+} and V^{4+}). In contrast, two-electron cycling of the metal center is present in the documented mechanism for the C_2H_2 cyclotrimerization. The C_2H_2 cyclotrimerization over the Ti atom and TiO molecule is also studied, and the documented mechanism applies in this case. The new mechanism is suggested to apply to reactions using titanium and vanadium oxides as catalysts.

1. Introduction

Benzene is used primarily as a solvent and a starting material in the synthesis of numerous chemicals. Thermal cyclization of three acetylene molecules to form benzene was first discovered in 1866.[1] However, temperatures higher than 400 °C are required,[2] even though this transformation is extremely exothermic (by about 6.19 eV)[3] at room temperature. This situation was greatly changed by using a nickel-containing catalyst ($NiBr_2$) as reported by Reppe et al. in 1948.[4] Since then, a variety of other transition-metal (Co, Ti, Ir, Rh, Pd, etc.) complexes have been found to homogeneously catalyze this reaction.[5−9] This reaction can also be heterogeneously catalyzed by supported metals such as Pd/MgO and Ni/SiO_2[10−12] and by metal oxides such as TiO_2[13] and V_2O_4/V_2O_5.[14]

To understand the mechanisms of the benzene formation from acetylene, single-crystal surfaces of various metals, bimetallic systems, and metal oxides under ultrahigh vacuum to atmospheric pressure conditions have been used as model catalysts;[15] Pd(111),[16] Cu(111),[17] Pd/W(211),[18] Sn/Pt(111),[19] reduced TiO_2-(001),[20,21] and so forth were found to be catalytic. Supported Pd_n clusters with $n = 1−30$ were also studied to selectively catalyze this reaction.[12,22,23]

The established mechanisms of the C_2H_2 cyclotrimerization in the homo- and heterogeneous catalytic processes are similar in most cases. A "common mechanism" of the C_2H_2 cyclotrimerization involves two important intermediates, (1) a metallacyclopentadiene complex formed from a metal center and two C_2H_2 monomers and (2) a complex formed by insertion or addition of the third C_2H_2 to the complex in (1).[5−7,10,12] The metal center is oxidized in the formation of the metallacyclopentadiene compound and reduced in the final benzene formation. The catalytic cycle involves transfer of two electrons from and to the metal center (two-electron cycling of the metal center). The "common mechanism" is supported by theoretical calculations.[24−26]

In addition to these condensed-phase studies, several investigations on the benzene formation from acetylene are carried out under the gas-phase conditions. Fe^+ and small iron clusters are catalytic toward the C_2H_2 cyclotrimerization.[27] The benzene formation from ionized acetylene van der Waals clusters in absence of catalyst has also been suggested.[28,29] The C_2H_2 cyclotrimerization process mediated by early second-row transition-metal atoms (Y, Zr, Nb, and Mo) is also facile, as reported in computational studies.[30] The gas-phase studies are important to have a general understanding of the C_2H_2 cyclotrimerization. Moreover, these studies are important to find alternative catalysts and possibly new mechanisms for the cyclotrimerization of C_2H_2 or, generally, of alkynes and their derivatives, which meets challenges in terms of chemo-, regio-, and enantioselectivity of the products.[6−9]

In this study, TiO_2 and VO_2 are taken as model catalysts for the C_2H_2 cyclotrimerization. From gas-phase (atomic level) studies, it is quite well-established that bare early transition metals are very active toward activation of very stable main group compounds, such as activation of the CO bond in CO_2 by Ti and V,[31] activation of CC and CH bonds in hydrocarbons by V, Nb, Ta, and their neutral and ionic clusters,[32−35] and so on. These investigations provide valuable mechanistic clues for important applications such as CO_2 transfer, CC coupling, and so forth.[36,37] However, from a practical point of view, it is inconvenient to handle bare early transition metals. Metal oxides

* To whom correspondence should be addressed. E-mail: shengguihe@iccas.ac.cn. Phone: 86-10-62536990. Fax: 86-10-62559373.

10.1021/jp711027z CCC: $40.75
Published on Web 03/19/2008

such as titanium and vanadium oxides are important stable forms of the early transition metals. Bulk TiO_2 and V_2O_4/V_2O_5 compounds are extensively used catalysts in industry and in laboratory.[22,38,39] The bulk TiO_2[21] has been found to be catalytic toward the C_2H_2 cyclotrimerization, and the V_2O_4/V_2O_5[14] are used as catalysts for the same process in applications such as ^{14}C dating. The atomic-level benzene formation mechanisms over these oxides are not well-understood. The TiO_2 and VO_2 molecules are thus used as model catalysts in motivation to have a possible mechanistic understanding.

This work is also motivated by a recent gas-phase experimental study employing a time-of-flight mass spectrometry on reactions of neutral vanadium oxide clusters with C_2H_2.[40] It is found that the VO_2 molecule reacts with C_2H_2 to form $VO_2C_2H_2$ and $VO_2C_4H_4$ at room temperature. It is noticeable that both the primary ($VO_2C_2H_2$) and secondary ($VO_2C_4H_4$) addition products are strongly observed, while the tertiary addition product $VO_2C_6H_6$ is not observed (or barely observed due to experimental uncertainty). This hints that $VO_2C_6H_6$ may be formed ($VO_2C_4H_4 + C_2H_2 \rightarrow VO_2C_6H_6$) as a reaction intermediate, but it is not detectable due to benzene formation ($VO_2C_6H_6 \rightarrow VO_2 + C_6H_6$). It is interesting to use theoretical computations to address this problem.

2. Computational Details

Density functional theory (DFT) calculations using the Gaussian 03 program[41] have been employed to study reactions of neutral MO_2 (M = Ti, V) with three C_2H_2 molecules step by step

$$MO_2 + C_2H_2 \rightarrow MO_2C_2H_2 \quad (1)$$

$$MO_2C_2H_2 + C_2H_2 \rightarrow MO_2C_4H_4 \quad (2)$$

$$MO_2C_4H_4 + C_2H_2 \rightarrow MO_2C_6H_6 \rightarrow MO_2 + C_6H_6 \quad (3)$$

In each step, the reaction path is followed from the ground state of the reactants. The reaction path calculations involve geometry optimization of various reaction intermediates and transition states (TSs) through which the intermediates transfer to each other. The TS optimizations are performed by using either the Berny algorithm[42] or the synchronous transit-guided quasi-Newton (STQN) method.[43,44] Vibrational frequencies are calculated to check that the reaction intermediates and the TSs have all positive and only one imaginary frequency, respectively. Intrinsic reaction coordinate (IRC) calculations[45,46] are also performed so that a TS connects two appropriate local minima in the reaction paths. The hybrid B3LYP exchange-correlation functional[47−49] is adopted. A contracted Gaussian basis set of triple-ζ valence quality[50] plus one p function for H, Ti, and V atoms and one d function for C and O atoms is used. The basis set is denoted as TZVP in the Gaussian 03 program.

To compare with the catalytic properties of TiO_2, the calculations for reactions of Ti and TiO with three C_2H_2 molecules are also performed. Some side reactions such as $VO_2C_4H_4 \rightarrow VO + C_4H_4O$ (furan) and $VO_2C_4H_4 \rightarrow VOC_4H_2 + H_2O$ are also considered. To interpret the gas-phase experimental results,[40] relative free energies at 298 K ($\Delta G_{298\,K}$) are reported in this study. Basis set superposition error (BSSE)[51] is not corrected in reporting all of the relative energies. Test calculations on species **1**/$TiO_2-C_2H_2$, **3**/$TiO_2C_2H_2-C_2H_2$, and **5**/$TiO_2C_4H_4-C_2H_2$ (see Figures 1 and 2 presented below) show that the BSSE corrections are about 0.02−0.03 eV, which are negligible. Cartesian coordinates, electronic energies, and vibrational frequencies for all of the optimized structures are available upon request.

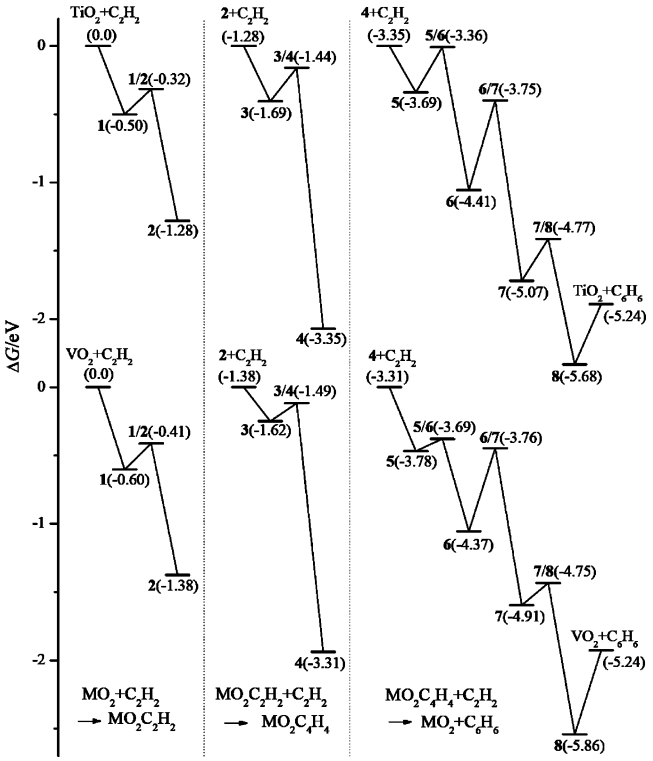

Figure 1. Potential energy profiles for reactions of $MO_2C_{2x}H_{2x} + C_2H_2$ (M = Ti, V and $x = 0, 1, 2$). The titanium (top panel) and vanadium (bottom panel) species are in the singlet and doublet spin multiplicities, respectively. An integer ***n*** is used to denote the reaction intermediate, and the two integer combination $\boldsymbol{n}_1/\boldsymbol{n}_2$ is used to denote the transition state that connects the reaction intermediates $\boldsymbol{n}_1$ and $\boldsymbol{n}_2$. The values in the parentheses are Gibbs free energies (in eV) at 298 K relative to $MO_2 + 3C_2H_2$

3. Results and Discussion

3.1. Accuracy of the Calculations. To gauge the validity of the B3LYP/TZVP method for calculating the thermodynamics of the reactions that involve bonding of Ti/V with C and O and C with C and O, some bond enthalpies are calculated and compared with available experimental data in literature.[52−58] The comparison is listed in Table 1. The bond enthalpies of Ti−O, V−O, and Ti−C_2, and C_6H_6 from three C_2H_2 molecules are computed within experimental uncertainties. The B3LYP/TZVP method underestimates bond enthalpies of OTi−O, OV−O, Ti−C_2, V−C_2, and CO by values (in eV) of 0.52, 0.47, 0.10, 0.33, and 0.31, respectively. In reaction 1 (see details in section 3.3), weakening of the OM═O double bond is accompanied by formation of O−C and M−C bonds. Due to error cancellation, it is expected that the accuracy of the computed relative energies is probably within $|0.52 - 0.10 - 0.31| = 0.11$ eV and $|0.47 - 0.33 - 0.31| = 0.17$ eV for species in $TiO_2 + C_2H_2$ and $VO_2 + C_2H_2$ reactions, respectively.

3.2. Overview of the Results. Figure 1 plots the potential energy profiles for TiO_2 and VO_2 reacting with three C_2H_2 molecules as in reactions 1−3. The structures and relative Gibbs free energies of the reaction intermediates and TSs are shown in Figures 2 and 3 for $TiO_2 + 3C_2H_2$ and $VO_2 + 3C_2H_2$, respectively. The three reactions 1−3 that finally produce benzene are all overall barrierless at room temperature. As a result, MO_2 (M = Ti, V) are good catalysts for the C_2H_2 cyclotrimerization in the gas phase. Ti and TiO are also found

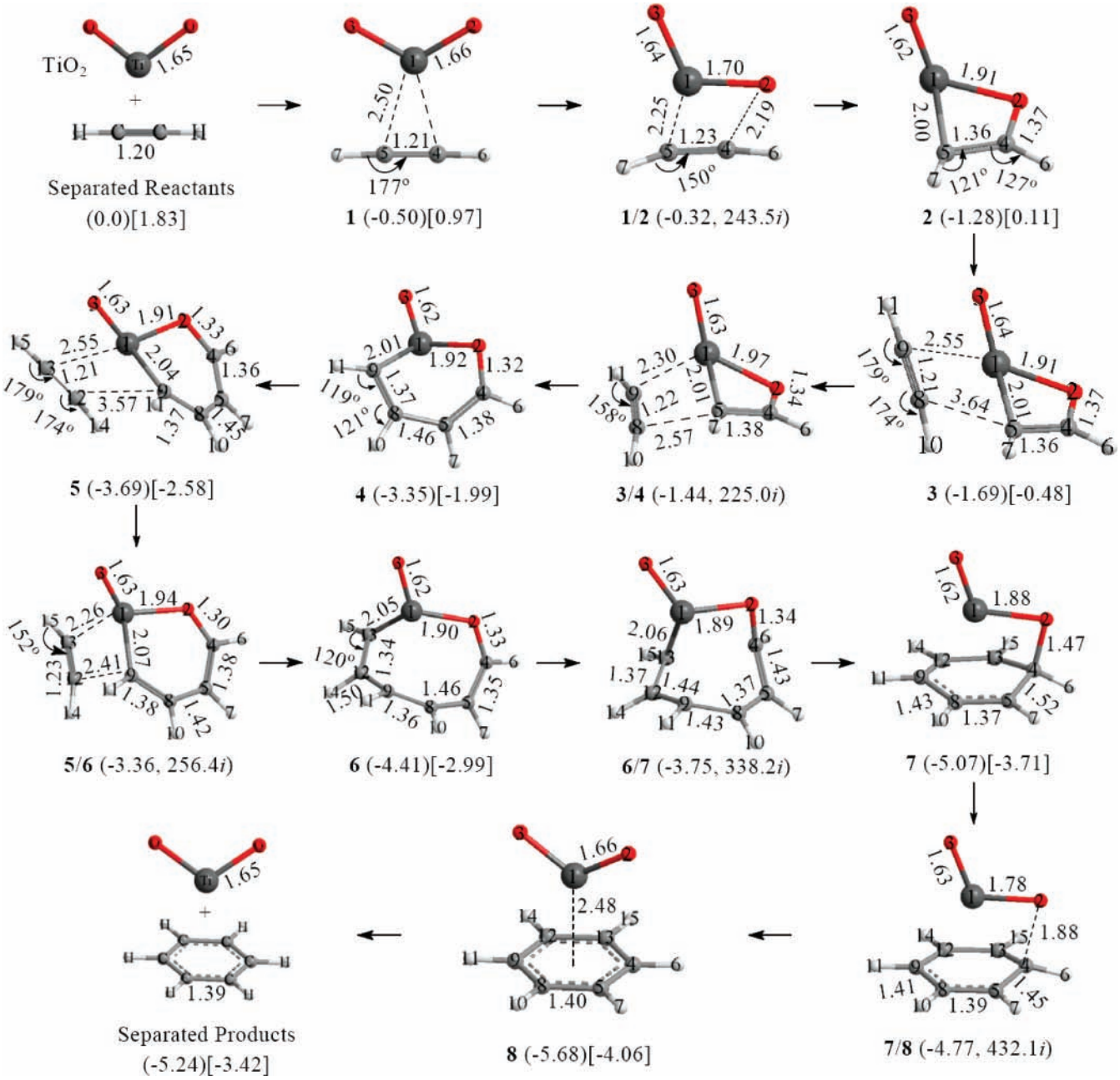

Figure 2. Structures of the titanium species in Figure 1. The free energies (in eV) of the singlet and triplet states relative to TiO_2 (singlet) + $3C_2H_2$ are given in the parentheses and square brackets, respectively. The imaginary frequencies (in cm^{-1}) of the singlet transition states are given after the energies in the parentheses. The bond lengths are given in 0.1 nm. Some HCC angles in deg are also given.

TABLE 1: A Comparison of Calculated and Experimental Enthalpy Changes (in eV) at 298 K for Some Selected Reactions (Superscripts Denote the Spin Multiplicities of the Species)

		expt.	
reaction	calc.	value	reference
$^3TiO \rightarrow {}^3Ti + {}^3O$	6.92	6.92 ± 0.09	52
$^4VO \rightarrow {}^4V + {}^3O$	6.34	6.44 ± 0.20	52
$^1TiO_2 \rightarrow {}^3TiO + {}^3O$	5.79	6.31 ± 0.15	52
$^2VO_2 \rightarrow {}^4VO + {}^3O$	5.25	5.72 ± 0.21	54
$^3Ti{-}C_2 \rightarrow {}^3Ti + {}^3C_2$	5.75	5.85 ± 0.17	55
$^4V{-}C_2 \rightarrow {}^4V + {}^3C_2$	5.60	5.93 ± 0.20	56
$^1CO \rightarrow {}^3C + {}^3O$	10.84	11.15 ± 0.01	57
$^1C_6H_6 \rightarrow 3\,^1C_2H_2$	6.20	6.19 ± 0.03	58

to be able to catalyze the benzene formation at room temperature. Figures 4 and 5 plot the potential energy profiles for the reactions involving Ti and TiO, respectively. The structures and relative free energies of the reaction intermediates are given in Figures 6, 7, and 8 for Ti + $3C_2H_2$ and TiO + $3C_2H_2$ reactions.

The ground states of TiO_2 and VO_2 are the singlet and the doublet, respectively. The structures of the reaction intermediates (**1**−**8** in Figures 1−3) with higher spin multiplicities (triplet and quartet) are also optimized. Their energies are given in the square brackets of Figures 2 and 3. The higher spin states are all above the corresponding lower spin states by at least 0.8 eV (**4** in Figure 3). The TS structures with higher spin multiplicities are not optimized. Their energies are all higher than the energies of the corresponding lower-spin TSs, as can be seen from the relative energies of the reaction intermediates (Figures 2 and 3). As a result, there is no curve crossing between the ground- and the exited-state reaction potential energy profiles (spin conversion[59]) for MO_2 + $3C_2H_2$ reactions. The triplet−singlet spin conversion exists in reactions Ti + $3C_2H_2$ and TiO + $3C_2H_2$. Ti has the triplet ground state. The optimized energies

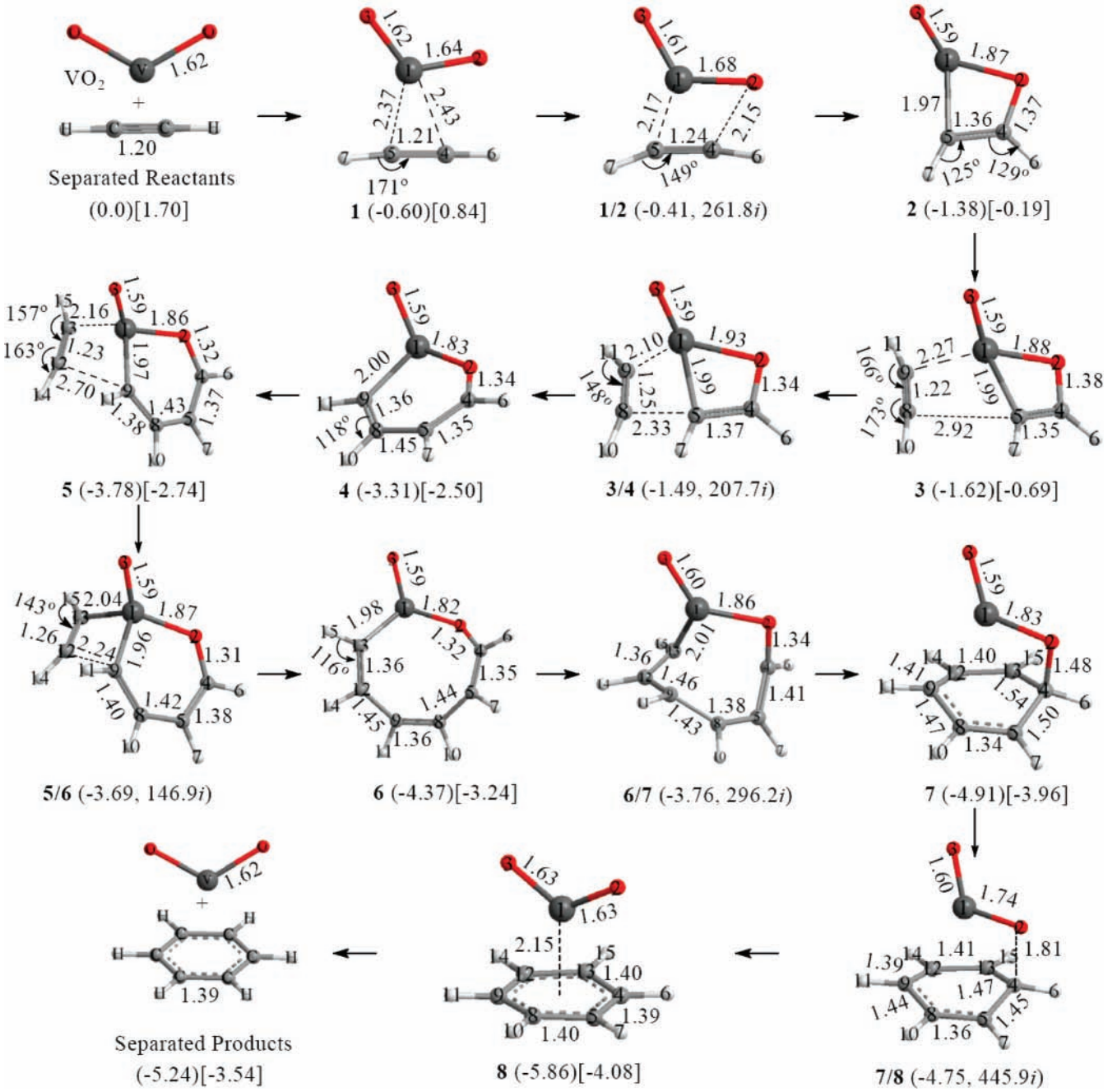

Figure 3. Structures of the vanadium species in Figure 1. The free energies (in eV) of the doublet and quartet states relative to VO_2 (doublet) + $3C_2H_2$ are given in the parentheses and square brackets, respectively. The imaginary frequencies (in cm^{-1}) of the doublet transition states are given after the energies in the parentheses. The bond lengths are given in 0.1 nm. Some HCC angles in deg are also given.

of the reaction intermediates and TSs with the singlet multiplicity are given in the square brackets of Figure 6. For simplicity, Figure 4 plots the reaction energy profile only for the triplet state since the reaction (benzene formation) can happen without considering mechanisms of the spin conversion. Both the triplet and singlet potential energy profiles are given in Figure 5 for TiO + $3C_2H_2$.

For reactions 1−3, many other possible reaction intermediates not shown in Figures 2 and 3 are also obtained. Figure S1 (Supporting Information) plots some typical structures and their relative free energies. No attempt has been made to determine how these species are formed from the separated reactants (MO_2 + xC_2H_2, x = 1, 2, 3), which involves locating many new TSs not listed in Figures 1−3. Figures S2 (Supporting Information) plots the reaction path that causes furan formation starting from structure **4** in Figure 3 ($VO_2C_4H_4$ → VO + C_4H_4O). Possible structures and free energies for an experimentally observed species VOC_4H_2[40] are given in Figure S3 (Supporting Information).

3.3. C_2H_2 Coordination and Activation. Figures 1−3 shows that for reactions 1, 2, and 3, the C_2H_2 molecule coordinates to $MO_2C_{2x}H_{2x}$ (x = 0, 1, and 2) through processes **1** → **1/2** → **2**, **3** → **3/4** → **4**, and **5** → **5/6** → **6**, respectively. The reacting C_2H_2 is weakly bonded in structures **1**, **3**, and **5** with binding energies of 0.24−0.60 eV that are determined by the free-energy differences [such as $\Delta G_{298\,K}(MO_2) + \Delta G_{298\,K}(C_2H_2) - \Delta G_{298\,K}(MO_2C_2H_2)$ for binding of MO_2 with C_2H_2] in Figure 1. It is noticeable that the free energies at 298 K are reported in all of the figures in this study. However, the binding energy is usually defined as the enthalpy change at 0 K, that is, $\Delta H_{0\,K}(A) + \Delta H_{0\,K}(B) - \Delta H_{0\,K}(AB)$ for the binding of species A with B. The binding energy defined by $\Delta G_{298\,K}$ will be lower than that

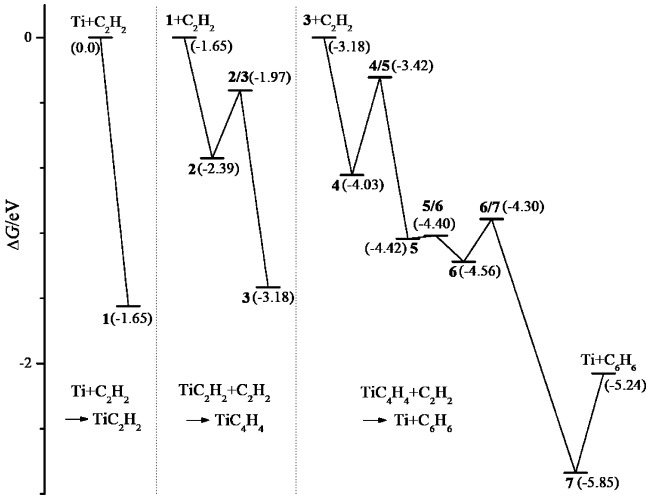

Figure 4. Potential energy profiles for reactions of $TiC_{2x}H_{2x} + C_2H_2$ ($x = 0, 1, 2$). The species are in the triplet spin multiplicity. An integer $\boldsymbol{n}$ is used to denote the reaction intermediate, and the two integer combination $\boldsymbol{n}_1/\boldsymbol{n}_2$ is used to denote the transition state that connects the reaction intermediates $\boldsymbol{n}_1$ and $\boldsymbol{n}_2$. The values in the parentheses are Gibbs free energies (in eV) at 298 K relative to $Ti + 3C_2H_2$.

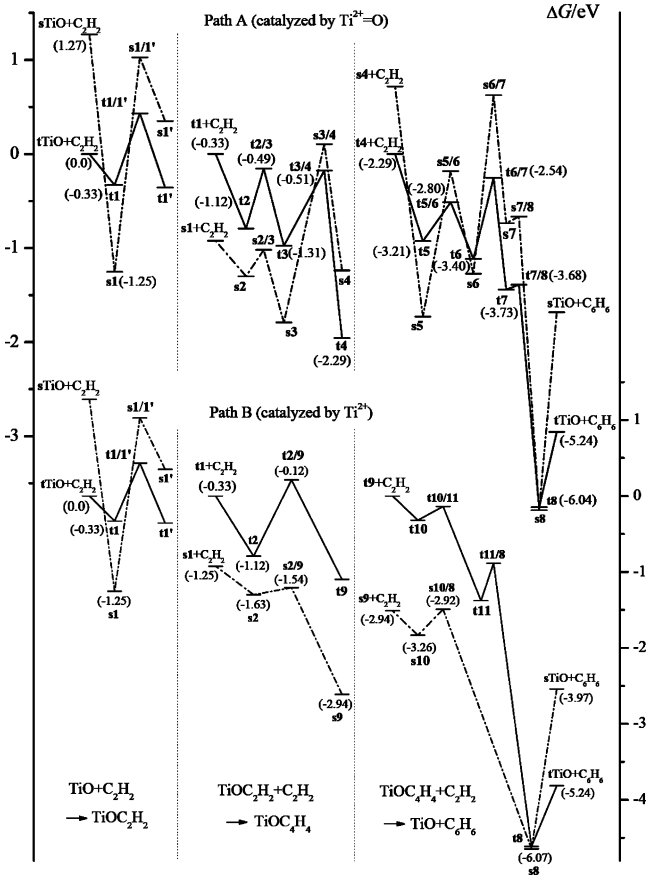

Figure 5. Potential energy profiles for reactions of $TiOC_{2x}H_{2x} + C_2H_2$ ($x = 0, 1, 2$). Reaction Path A (top panel) and Path B (bottom panel) with species in both the singlet (**s-** such as **s**TiO and **s1**) and triplet (**t-** such as **t**TiO and **t1**) spin multiplicities are given. An integer $\boldsymbol{n}$ is used to denote the reaction intermediate, and the two integer combination $\boldsymbol{n}_1/\boldsymbol{n}_2$ is used to denote the transition state that connects the reaction intermediates $\boldsymbol{n}_1$ and $\boldsymbol{n}_2$. The values in parentheses are Gibbs free energies (in eV) at 298 K relative to TiO (triplet) $+ 3C_2H_2$.

defined by $\Delta H_{0\,K}$ due to entropy loss after forming AB from the free A and B at 298 K. The binding energies defined by $\Delta H_{0\,K}$ are (in eV) 0.83/0.95 (**1**), 0.78/0.65 (**3**), and 0.73/0.90 (**5**) for $TiO_2C_{2x}H_{2x}/VO_2C_{2x}H_{2x}$. These energies are 0.3−0.4 eV higher than the free-energy differences read directly from Figure 1.

The weakly bonded species **1**, **3**, and **5** are converted to species **2**, **4**, and **6**, respectively, by overcoming barriers (0.09−0.33 eV) that are less than the corresponding binding energies (0.24−0.60 eV, defined by $\Delta G_{298\,K}$). The C_2H_2 moiety is strongly bonded to $MO_2C_{2x}H_{2x}$ ($x = 0$, 1, and 2) by forming MC and CO ($x = 0$) or CC ($x = 1$, 2) bonds. Additional net free energies of 0.59−1.69 eV are released. The C_2H_2 is only slightly activated in **1**, **3**, and **5**, which can be seen from the small binding energies (0.24−0.60 eV, defined by $\Delta G_{298\,K}$), long M−C distances (0.216−0.255 nm), a slight increase of the CC bond lengths (0.121−0.123 nm, 0.120 nm in free C_2H_2), and nearly 180° CCH bond angles. The reacting C_2H_2 gets fully activated in **2**, **4**, and **6**, which is reflected by the large binding energies (1.06−2.07 eV), short M−C distances (0.197−0.205 nm), and significant change of the CC bond lengths (0.134−0.137 nm) and HCC bond angles (116−129°) with respect to the free C_2H_2 molecule.

It is noticeable that the CC bond lengths of the activating C_2H_2 moiety in TSs **1/2**, **3/4**, and **5/6** (Figures 2 and 3) are very close to (or slightly longer than) the corresponding CC bond lengths in species **1**, **3**, and **5**, while the CC bond length values in **2**, **4**, and **6** are significantly longer. The IRC[45,46] calculations have verified that each TS $\boldsymbol{n}_1/\boldsymbol{n}_2$ connects appropriate intermediates $\boldsymbol{n}_1$ and $\boldsymbol{n}_2$ in our study. The imaginary vibrational frequency of each TS is also given in the parentheses of the figures. For the easiest conversion (**5** → **5/6** → **6** in Figure 3, 0.09 eV barrier), the frequency (in i cm^{-1}) is the smallest (146.9), while for the others, the values are all above 200 cm^{-1}. This further tells that the located TSs are correct. It can be seen in Figures 2 and 3 that the changes of the CCH bond angles in these TSs are significant with respect to the structures of intermediates **1**, **3**, and **5**. This indicates that the character of the TSs may be understood as overcoming the barriers in changing the orbital hybridization ($sp^1 \rightarrow sp^2$ from **1**, **3**, and **5** to **2**, **4**, and **6**, respectively) of the carbon atoms in the activating C_2H_2 moiety. The change of orbital hybridization ($sp^1 \rightarrow sp^2$) does not require lengthening of the CC bond, although it causes a significant lengthening after the change. This rationalizes the above-mentioned CC bond length issue for the TSs **1/2**, **3/4**, and **5/6**.

We noticed that the benzene formation from three C_2H_2 molecules over Pd atoms and Pd clusters has been studied in detail by Pacchioni et al.[22,26] For the unsupported Pd atom system, the third C_2H_2 molecule binds weakly to the reaction intermediate (PdC_4H_4) with a binding energy of less than 0.3 eV.[22b] However, for the supported (on MgO thin film) Pd system, the third C_2H_2 binds to PdC_4H_4 strongly due to electronic modification of Pd induced by interaction with the surface defect.[22c] The third C_2H_2 is strongly activated in the supported system, while it is not activated in the unsupported system. The free Pd atom is thus not considered a catalyst for the benzene formation. In our study, there is a similar situation that the C_2H_2 moiety is not strongly bonded and thus not fully activated in structures **1**, **3**, and **5** in Figures 1−3. However, according to the calculations, the overall barrierless conversions (**1** → **1/2** → **2**, **3** → **3/4** → **4**, and **5** → **5/6** → **6**) of the weakly bonded to the strongly bonded species indicate that the C_2H_2 full activation over $MO_2C_{2x}H_{2x}$ ($x = 0-2$) is not subject to any thermodynamic and kinetic difficulties. Moreover, the interaction between C_2H_2 and $MO_2C_{2x}H_{2x}$ (binding energy = 0.65−0.90 eV, defined by $\Delta H_{0\,K}$) is stronger than that between C_2H_2 and

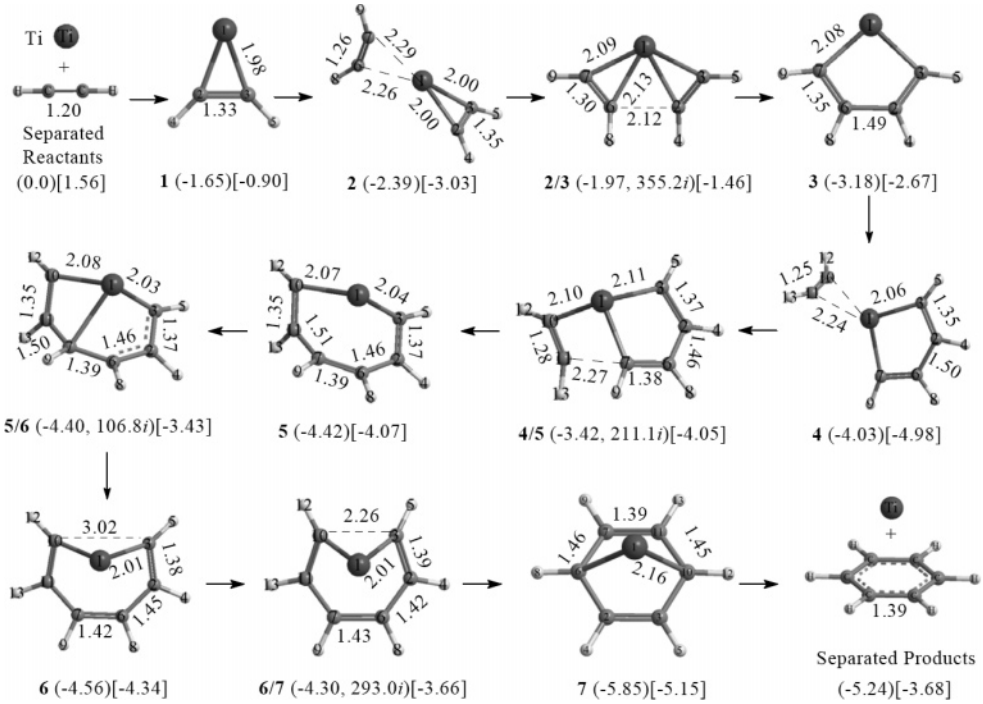

Figure 6. Structures of the species in Figure 4. The free energies (in eV) of the triplet and singlet states relative to Ti (triplet) + $3C_2H_2$ are given in the parentheses and square brackets, respectively. The imaginary frequencies (in cm^{-1}) of the triplet transition states are given after the energies in the parentheses. The bond lengths are given in 0.1 nm.

the free PdC_4H_4 (binding energy < 0.3 eV). We conclude that the initial coordination of C_2H_2 to $MO_2C_{2x}H_{2x}$, which is considered to be important for the benzene formation,[22] is strong enough to make the whole procedure be in progress.

In Figure 2, it is shown that although Ti in TiO_2 is saturated by two O atoms (similar for V in VO_2, which is nearly oxygen saturated), it can still coordinate C_2H_2 though weak bonding. A NBO analysis[60] indicates that the interaction between C_2H_2 and TiO_2 in **1** of Figure 2 is through weak electron donation from the HOMO (π) of C_2H_2 to the vacant d orbital of Ti. Similar situations are found for **3** and **5** in Figure 2 as well as for **1**, **3**, and **5** in Figure 3. In the process of **1** → **1/2** → **2**, the C_2H_2 activation is actually through one of the MO double bonds in MO_2 rather than the single metal center of Ti^{4+} or V^{4+}. This is evident by the character of the double MO bond (length = 0.164−0.166 nm) in **1** and single MO bond (length = 0.187−0.191 nm) in **2**. We can see that formation of **2** involves at least four processes together, formation of MC and CO bonds and partial cleavage of CC (triple CC → double CC) and MO (double MO → single MO) bonds. Because of the play of early transition metals (Ti^{4+} and V^{4+}), the net thermodynamics of this process is not critical. It is subject to 0.18−0.19 eV reaction barriers that can be overcome by the binding energies released from the structure **1** formation. We can see that as one of the MO bonds becomes a single bond in **2**, two electrons are transferred from the catalyst (MO double bond) to form bonds with the C_2H_2 moiety. The metal center (M^{4+}) is still in its +4 oxidation state.

The Zhou group studied the reaction of TiO_2 with C_2H_2 under matrix isolation conditions (11−28 K) by the FT-IR technique.[61] The species **1** ($TiO_2C_2H_2$) is identified, with no indication of **2** being observed, although **2** is more stable than **1** and the calculated IR spectrum of **2** is quite different from that of **1**. This indicates that the binding energy (~0.5 eV) through formation of **1** is quickly dissipated to the low-temperature matrix and the species is stabilized as **1**. Because a low barrier (0.18 eV at 298 K) is predicted for the $TiO_2C_2H_2$ **1** → **1/2** → **2** process, there is a possibility that **2** can be observed. The lifetime (k^{-1}) of species **1** can be estimated by using a rate equation $k = \nu \exp(-\Delta G/k_bT)$, where k_b is the Boltzmann constant, T is the temperature, ΔG is the activation energy (0.115 eV at $T \approx 0$), and ν can be estimated by the absolute value (243.5 cm^{-1} = 7.30 THz) of the imaginary frequency of **1/2**. A lifetime of $k^{-1} = 6.83 \times 10^7$ s = 1.90×10^4 h is obtained for $T = 28$ K. This explains the absent observation of **2** in the matrix isolation experiments and thus verifies the existence of the TS **1/2**. In contrast, the lifetime of **1** at room temperature (298 K) will be only 0.15 ns by a similar estimation. To observe **2** under the low-temperature condition in 1 h (k^{-1} = 1 h), T = 35.3 K is required.

After formation of **2**, which contains a four-membered ring (−O−M−C═C−, Figures 2 and 3), the reaction 2 proceeds through insertion of the second C_2H_2 into the MC bond in **2** to form species **4** with a six-membered ring (−O−M−C═C−C═C−). A CC bond (length = 0.145−0.146 nm) with σ character between the two C_2H_2 moieties is formed. This insertion process is repeated in reaction 3, which results in species **6** with an eight-membered ring (−O−M−C═C−C═C−C═C−). The DFT study in this work shows that C_2H_2 activation over MO_2 is different from that over other transition-metal-containing compounds in the literature,[24,26,30] where the formation of species with the five- and seven-membered rings (−M−C═C−C═C−, −M−C═C−C═C−C═C−) are identified.

3.4. C_6 Aromatic Ring Formation. The final benzene formation proceeds with contraction of the eight-membered ring (**6** in Figures 2 and 3). This process is subject to a barrier of 0.66 eV for $TiO_2C_6H_6$ and 0.61 eV for $VO_2C_6H_6$. This contraction results in a species **7** with a C_6 ring that is attached to MO_2 through a CO bond. Breakage of this CO bond is subject to a small barrier (0.17−0.31 eV) and leads to a species **8**, which is the association compound of benzene with the original MO_2 catalyst. It takes an energy of 0.44−0.61 eV to boil off benzene from MO_2. The DFT result shows that the contraction of the eight-membered ring that results in the last CC σ bond in the

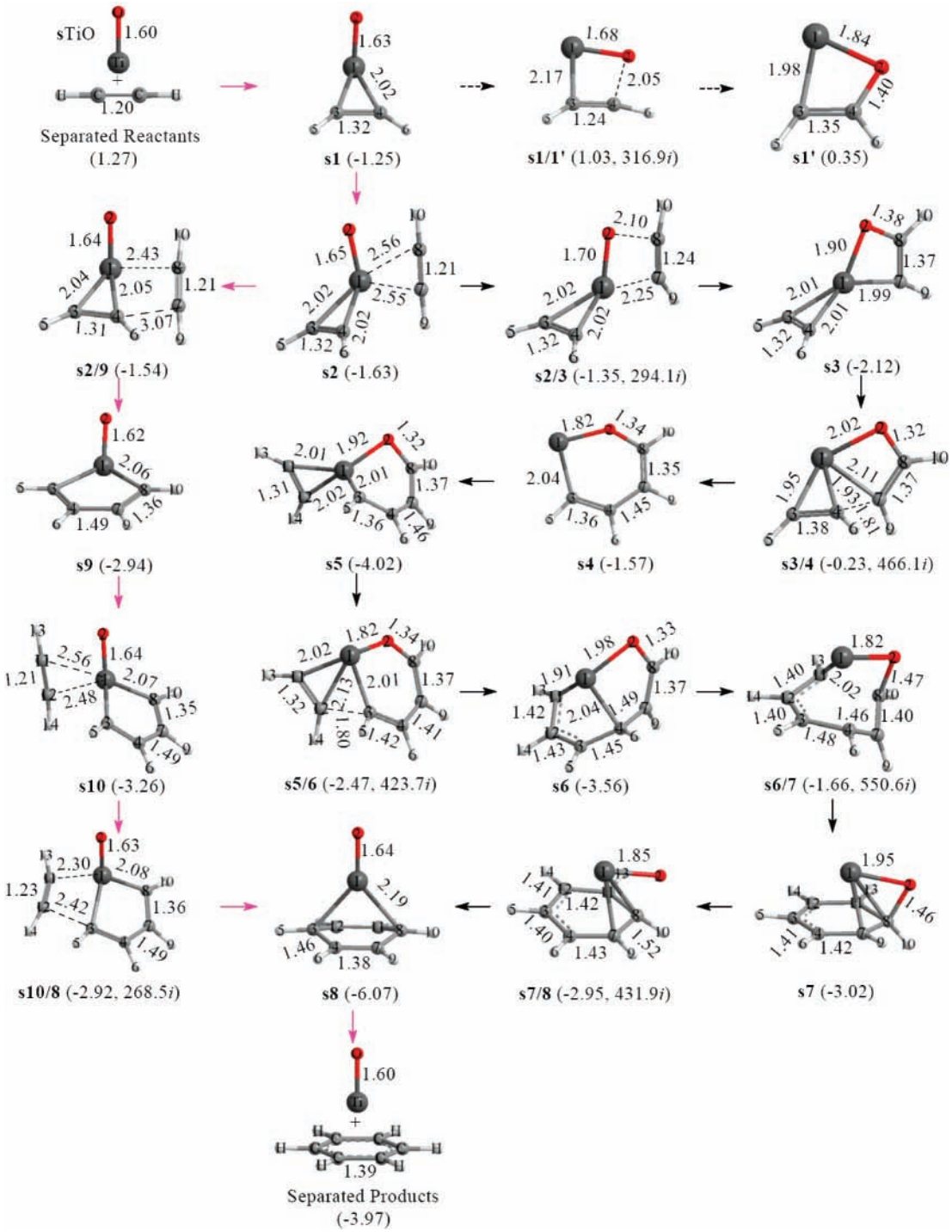

Figure 7. Structures of reaction species with singlet spin multiplicity in Figure 5. The free energies (in eV) relative to TiO (triplet) + $3C_2H_2$ are given in the parentheses. The imaginary frequencies (in cm^{-1}) of the transition states are given after the energies in the parentheses. The bond lengths are given in 0.1 nm. Pink arrows indicate a kinetically favorable reaction path.

C_6 ring is the most difficult step (with the highest barrier). This can be taken as the rate-limiting step for C_2H_2 cyclotrimerization over MO_2. The stable aromatic C_6 ring formation (**6** → **6/7** → **7**, **7** → **7/8** → **8**) is thermodynamically very favorable because each step results in a net energy release (Figure 1). Figure 9 plots some molecular orbitals (MOs) and their energies of $VO_2C_6H_6$ that correspond to three typical MOs of benzene (two framework σ and one delocalized π MO). The two σ MOs of benzene are in good shape in **6** and are almost formed after the eight-membered ring contraction (**6** → **6/7** → **7**). For the π molecular orbital, it involves relatively more electron distribution around the VO_2 moiety in species **6**, **6/7**, and **7**. The molecular orbital energy decreases in the process of the aromatic C_6 ring formation (**6** → **7** → **8**, and **6/7** → **7/8**). This reflects the high stability of the C_6 ring. As can be seen from the bond length change of the reacting MO bond in Figures 2 and 3, the MO double bond gets cycled in the final C_6 aromatic ring formation (**7** → **7/8** → **8**).

3.5. TiO_2 versus VO_2. In Figures 1−3, TiO_2 and VO_2 show very similar catalytic behavior in the process of the C_2H_2 cyclotrimerization. However, one more electron in VO_2 does cause differences in the details of the reaction mechanism. The first difference is that the coordination/activation of C_2H_2 over $TiO_2C_{2x}H_{2x}$ becomes more and more difficult as x increases

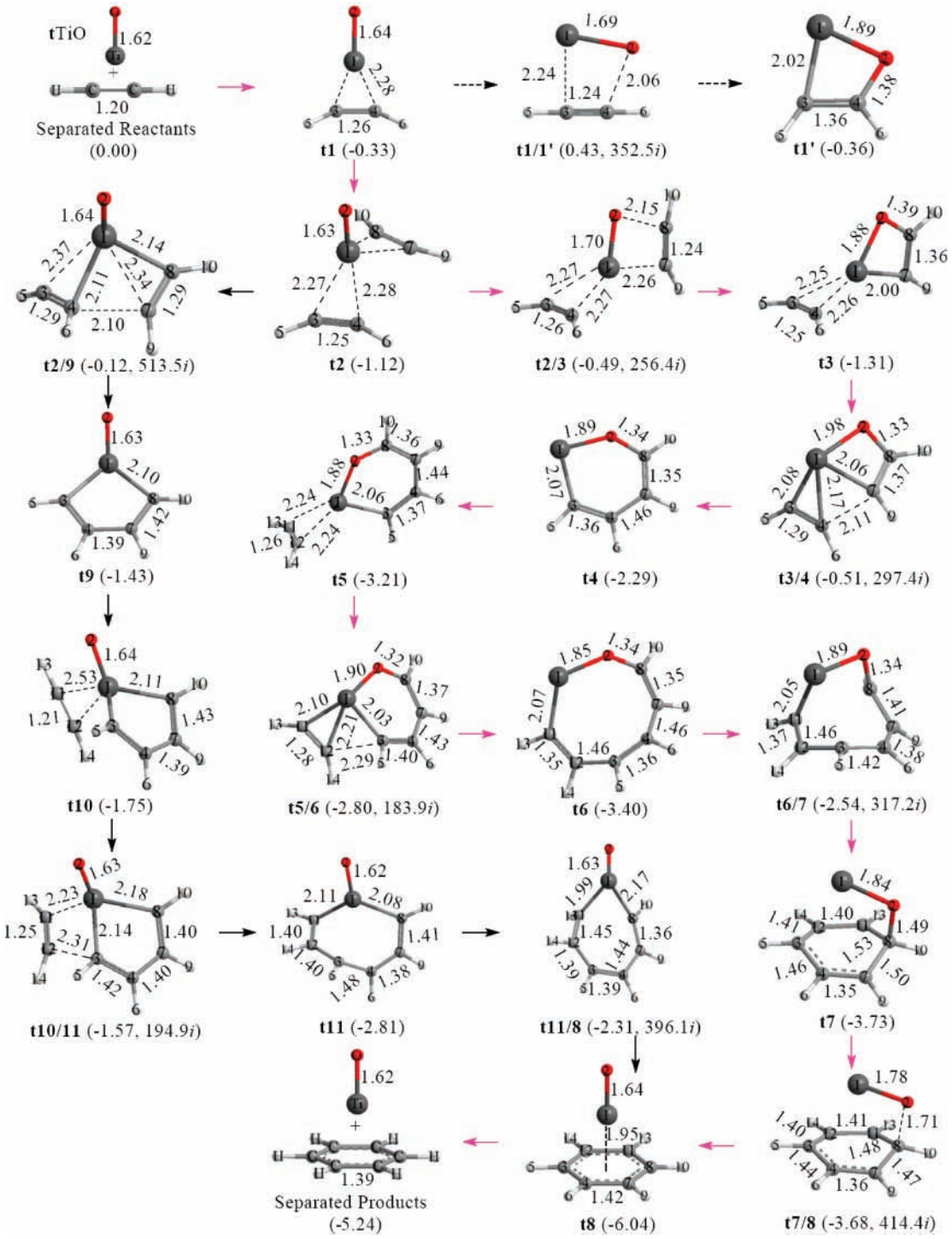

Figure 8. Structures of reaction species with triplet spin multiplicity in Figure 5. See caption of Figure 7 for explanation.

(from 0 to 2). This is evident from the increase of the ΔG values ($-0.32 \rightarrow -0.16 \rightarrow -0.01$ eV) of the first TS in reactions 1−3. In contrast, the corresponding change of ΔG values for vanadium compounds is $-0.41 \rightarrow -0.12 \rightarrow -0.38$ eV. The coordination/activation of the third C_2H_2 molecule is more facile than that of the second C_2H_2 over vanadium compounds. The second difference is that all of the activation steps ($\boldsymbol{n}_1 \rightarrow \boldsymbol{n}_1/\boldsymbol{n}_2 \rightarrow \boldsymbol{n}_2$) have smaller (more or less) barriers in vanadium species than those in titanium species. This is clear from the energy profiles in Figure 1. It is expected that one of the five valence electrons from vanadium ($4s^23d^3$) in VO_2 is free of bonding. This "free" electron makes VO_2 more catalytic than TiO_2, which has no such electron.

3.6. TiO_2 versus Ti and TiO. Figures 4 and 6 show that the C_2H_2 cyclotrimerization over the Ti bare atom is thermodynamically and kinetically favorable. The reaction mechanism is very similar to that over the Zr atom in ref 30. It is also consistent with the "common mechanism"[24−26] over a metal complex; the cyclotrimerization involves metal-containing intermediates with five- and seven-membered rings (**3**, **5**, **6** in Figure 6), and the process of two-electron cycling over the metal center is present. Because Ti^{4+} in TiO_2 is oxygen-saturated and two-electron cycling over Ti^{4+} is not possible, the Ti^{4+} center itself cannot catalyze the C_2H_2 cyclotrimerization. The C_2H_2 cyclotrimerization over TiO_2 is thus catalyzed by one of the TiO bond, as discussed previously. It becomes interesting to see the situation

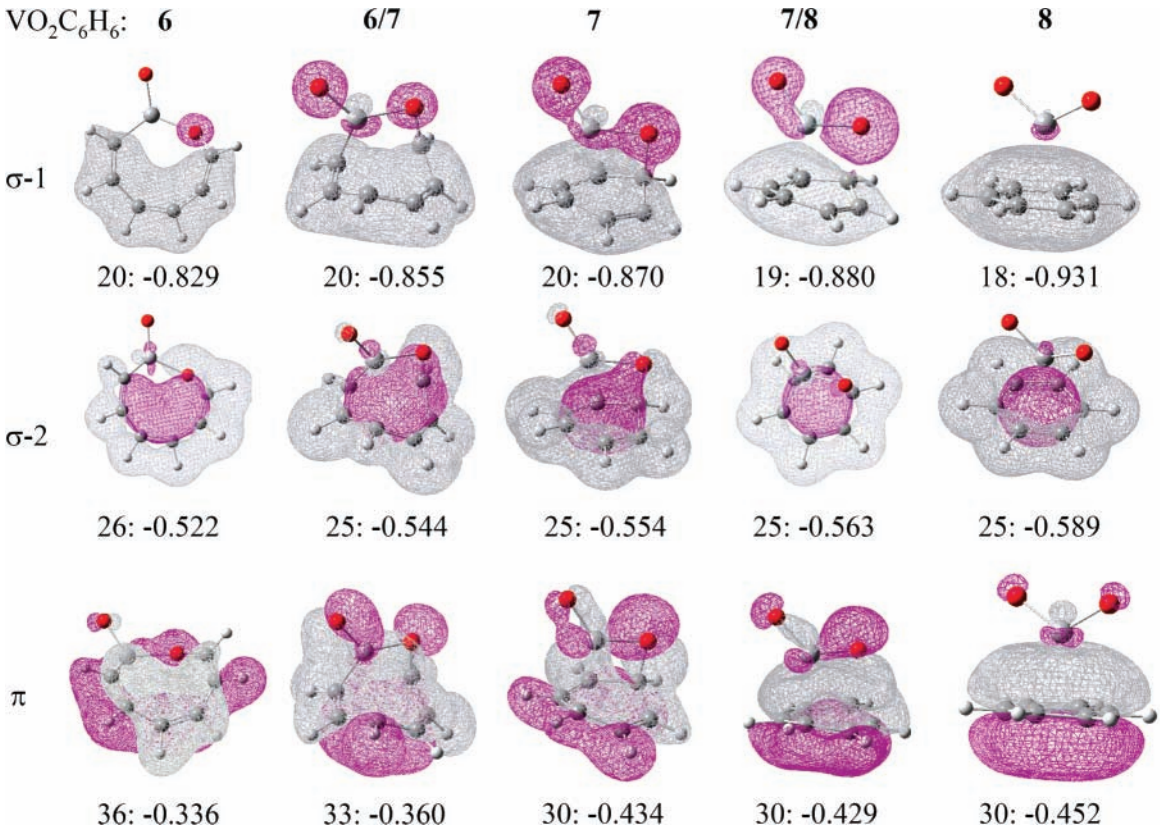

Figure 9. Molecular orbitals (MOs) of $VO_2C_6H_6$ (species **6**, **6/7**, **7**, **7/8**, and **8** in Figure 3) that correspond to three typical MOs of benzene. Under each MO, n and E_n are in the form of n: E_n denotes the nth α MO and its energy in Hartree, respectively.

over the TiO molecule where it is possible that the C_2H_2 cyclotrimerization would be catalyzed by both the Ti^{2+} center and the TiO bond.

TiO has a triplet ground state. In the reaction with C_2H_2 molecules, if an additional two Ti−C bonds are formed, it is expected that the species in the form of O═Ti═($C_{2x}H_{2x}$) would have a singlet ground state. We present in Figures 5, 7, and 8 the reactions of TiO with C_2H_2 molecules in the both triplet and singlet multiplicities. The first C_2H_2 approaches TiO in the triplet spin state from the metal side to form species **t1** directly or **s1** by spin conversion.[59] It is noticeable that **s1** has been identified in a matrix isolation experiment.[62] Formation of a four-membered ring structure (**t1′** and **s1′**) is subject to significant overall barriers. As a result, the second C_2H_2 coordination at room temperature is through interaction with **s1** and un-spin-converted **t1** rather than that with **t1′** and **s1′**. Species **t4** (Figure 8) with a six-membered ring (−Ti−O−C═C−C═C−) and **s9** (Figure 7) with five-membered ring (−Ti−C═C−C═C−) can be formed overall barrierlessly from **t1** + C_2H_2 and **s1** + C_2H_2, respectively. Benzene formation from **t4** + C_2H_2 and from **s9** + C_2H_2 is subject to no and tiny overall barriers, respectively. In **t4** + C_2H_2, a species (**t6** in Figure 8) with an eight-membered ring (−Ti−O−C═C−C═C−C═C−) is located in the reaction path. A C_2H_2 addition rather than the insertion intermediate (**s8** Figure 7) is found in the **s9** + C_2H_2 reaction. From Figures 5, 7, and 8, it can be concluded that both the Ti^{2+} center and the TiO bond in the TiO molecule are capable of catalyzing the C_2H_2 cyclotrimerization at room temperature according to the calculation.

There are obvious differences between the catalysis by the TiO bond over TiO and TiO_2 molecules, although the overall processes are similar. The first difference exists in the thermodynamics in the process of TiO covalent bonding with the C_2H_2 moiety (**t1** → **t1/1′** → **t1′** in Figures 5 and 8 vs **1** → **1/2** → **2** in Figures 1 and 2). The formation of **2** in Figure 2 results in a net energy release of 1.28 eV, while the energy release is only 0.36 eV in the formation of **t1′** in Figure 8. This can be understood by considering the effect of the "free" (nonbonded) electrons in the TiO molecule; due to nonbonded electrons in the TiO molecule, electron transfer from the C_2H_2 moiety to form bonds with TiO is less favorable than the transfer to TiO_2. In Figure 2, the length of the "free" TiO bond is shortened from 0.165 (free TiO_2) to 0.162 nm (structure **2**), indicating a strengthening of this TiO bond due to some electron donation from the C_2H_2 moiety. For a similar reason, the Ti−C and C−O bond lengths and the change of the reactive TiO bond length with respect to that of the free molecule in $TiO_2C_2H_2$ **2** are all (more or less) shorter or smaller than the corresponding values in **t1′**. All of these result in a higher (by about 1 eV) net energy release in the formation of **2** than that in the formation of **t1′**. This difference of thermodynamics is kept in the formation of the species with six- and eight-membered rings (**t4** and **t6** in Figure 8 vs **4** and **6** in Figure 2).

The second difference is that the formation of the eight-membered ring species $TiO_2C_6H_6$ **6** is less favorable than the formation of **t6** ($TiOC_6H_6$), as reflected by the relative free energies of the TSs **5/6** and **t5/6** (−0.01 eV vs −0.51 eV). This is consistent with the discussion in section 3.5; for a vanadium species that has one nonbonded electron, it is easier to coordinate/activate the third C_2H_2 molecule than it is for a titanium species that has no such electron.

3.7. Consideration of Related Gas-Phase Reactions of Neutral Vanadium Oxide Clusters. The reactions of C_2H_2 with a series of neutral vanadium oxide clusters in the gas phase have been studied recently.[40] Both $VO_2C_2H_2$ and $VO_2C_4H_4$ are clearly observed under near-room-temperature conditions. This verifies that VO_2 can react with two C_2H_2 molecules step by step in the gas phase. The DFT results shown in Figures 1 and

3 provide details of how the two products are formed in the gas-phase reactions. The DFT calculations predict that the binding energies of VO_2 with C_2H_2 and $VO_2C_2H_2$ with C_2H_2 are high (1.38 and 1.94 eV, respectively). It has been discussed[35] that a high binding energy corresponds to a long lifetime of the metastable collision complex ($VO_2C_2H_2$* and $VO_2C_4H_4$*). As a result, it is experimentally possible to observe the association products $VO_2C_2H_2$ and $VO_2C_4H_4$ due to stabilization of $VO_2C_2H_2$* and $VO_2C_4H_4$* through sufficient collisions with the helium bath gas in the experiment.

The DFT study of the $VO_2C_4H_4 + C_2H_2 \rightarrow VO_2 + C_6H_6$ reaction gives one interpretation for the absent observation of $VO_2C_6H_6$ because $VO_2C_6H_6$ (**8** in Figure 3) serves as a reaction intermediate that can fall apart into VO_2 and C_6H_6. Moreover, the binding energy between VO_2 and C_6H_6 is relatively low (0.61 eV). The high energy (2.54 eV) released in the $VO_2C_4H_4 + C_2H_2 \rightarrow VO_2C_6H_6$ (**8**) process drives a fast unimolecular reaction $VO_2C_6H_6$ (**8**) $\rightarrow VO_2 + C_6H_6$. These two points further support the interpretation that $VO_2C_6H_6$ will not be observed due to its short lifetime under the gas-phase conditions. The DFT calculations partly supported by the experiments predict that benzene formation from C_2H_2 can really be catalyzed by the neutral VO_2 cluster under room-temperature gas-phase conditions. Further experimental measurements focusing on detecting C_6H_6 and using different concentrations of C_2H_2 are likely to demonstrate an example of gas-phase catalysis over neutral transition-metal oxide clusters. It is noticeable that many excellent examples of gas-phase catalysis over ionic clusters have been documented,[63−65] while neutral cluster catalysis is almost neglected.

Two side channels involving formation of stable products (furan and water) in the reaction of $VO_2C_2H_2$ with C_2H_2 are also considered

$$VO_2C_2H_2 + C_2H_2 \rightarrow VO + C_4H_4O \quad (4)$$

$$VO_2C_2H_2 + C_2H_2 \rightarrow VOC_4H_2 + H_2O \quad (5)$$

Figure S2 (Supporting Information) shows that reaction 4 is exothermic if spin conversion[59] causes formation of the quartet VO. However, there is a significant overall barrier (0.42 eV) in the five-membered ring formation (**q4 → q4/15 → q15**) even if the spin conversion is considered. Figure S3 (Supporting Information) lists possible structures of VOC_4H_2 and the corresponding change of free energies (ΔG) for reaction 5. Structure **3** with doublet spin multiplicity has the lowest energy and the corresponding $\Delta G = 0.31$ eV. In the gas-phase experiment,[40] a weak product mass peak that corresponds to VOC_4H_2 is observed in reactions of C_2H_2 with neutral vanadium clusters. Reaction 5 could cause formation of VOC_4H_2, considering that $VO_2C_2H_2$ carries some unquenched binding energy ($\geq$0.31 eV) released in reaction 1. We have made no attempt in this study to determine a possible reaction path for $VO_2C_2H_2 + C_2H_2 \rightarrow H_2O +$ **3** (Figure S3, Supporting Information) due to complications of transferring at least two hydrogen atoms in the reaction. Considering the thermodynamic and kinetic (barriers and spin conversion) difficulties for reactions 4 and 5 and the observation of strong mass signal for $VO_2C_4H_4$, we conclude that reactions 4 and 5 are only possible minor side channels in the reactions of VO_2 with C_2H_2 molecules.

3.8. Consideration of the C_2H_2 Cyclotrimerization in Related Condensed-Phase Catalysis. Previous experimental studies[20,21] found that the reduced TiO_2(001) surface is catalytic toward the C_2H_2 cyclotrimerization. The surface Ti^{2+} sites are considered to be catalytically active. The reactions are suggested to proceed with mechanisms similar to those over the Ti atom (Figures 4 and 6) or TiO molecule (path B with singlet multiplicity in Figures 5 and 7) in this study. Although it is unnecessary to use new mechanisms to explain this surface chemistry, our DFT study does suggest that there is an alternative C_2H_2 cyclotrimerization mechanism; the TiO bond in the form of Ti^{2+}═O and Ti^{4+}═O is capable of catalyzing this reaction.

The new mechanism (Ti^{4+}═O and V^{4+}═O catalysis) of the C_2H_2 cyclotrimerization over TiO_2 and VO_2 molecules may be considered in understanding the results in other related condensed-phase catalysis. Vanadium oxide catalysts are used to convert C_2H_2 to benzene, which is a scintillation counting medium in ^{14}C dating. Vanadium oxides (treated with O_2 at 673 K) with only surface V^{4+} and V^{5+} species are catalytic toward this reaction at room temperature.[14] Meanwhile, TiO_2 powder (outgassed and then heated with O_2 at 773 K) with only surface Ti^{4+} species is also able to catalyze the C_2H_2 cyclotrimerization at room temperature.[13] Due to the involvement of two-electron cycling in the general mechanism of the C_2H_2 cyclotrimerization, surface Ti^{4+}, V^{4+}, and V^{5+} centers themselves are incapable of catalyzing the reaction. On the basis of the DFT study in this work, we thus suggest that surface species Ti^{4+}═O, V^{4+}═O, and possibly V^{5+}═O catalyze the C_2H_2 cyclotrimerization over nonreduced titanium and vanadium oxide catalysts.

The C_2H_2 cyclotrimerization is the simplest model process of the [2 + 2 + 2] cyclotrimerization of alkynes and their derivatives. The [2 + 2 + 2] cyclotrimerization is a very important process to synthesize organic molecules with chemo-, regio-, and enantioselectivity.[6−9] The documented mechanisms in most cases are similar; the catalytic reactions proceed over a single metal center that facilitates the two-electron cycling involved in the C_6 aromatic ring formation. The new mechanism (alkynes cyclotrimerization over the MO double bond, where M is an early transition metal) may be considered and used to produce organic molecules with good chemo-, regio-, and enantioselectivity, which is hard to achieve with the conventional mechanism.

4. Conclusion

Benzene formation from three C_2H_2 molecules over MO_2 (M = Ti and V) model catalysts is predicted to be highly favorable at room temperature, thermodynamically and kinetically. The calculated results can be tested in experiments such as the detection of benzene by mass spectrometry and the detection of reaction intermediates by low-temperature matrix isolation spectroscopy under related reaction conditions. The coordination and activation of C_2H_2 molecules is through the MO double bond in MO_2. The activation of C_2H_2 results in species with four-, six-, and eight-membered rings that contain metal and oxygen atoms. The rate-limiting step of the catalytic cycle is the contraction of the eight-membered ring that causes the formation of the C_6 ring. The cycling of two electrons from and to the catalyst in the catalytic process is through the MO bond (double → single → double) rather than the metal center. This suggests new mechanisms in condensed-phase catalysis of the C_2H_2 cyclotrimerization over early transition-metal oxides such as titanium and vanadium oxides. VO_2 that has one nonbonding electron is more catalytic than TiO_2 toward the C_2H_2 cyclotrimerization.

Acknowledgment. This work was supported by the Chinese Academy of Sciences (Hundred Talents Fund), the National Natural Science Foundation of China (No. 20703048), and the 973 Programs (Nos. 2006CB932100 and 2006CB806200).

Supporting Information Available: Stable structures of $MO_2C_{2x}H_{2x}$ ($x = 1$, 2, and 3) not shown in Figures 2 and 3 (Figure S1); structures of reaction species involved in $VO_2C_4H_4 \rightarrow VO + C_4H_4O$ (Figure S2); and optimized structures of VOC_4H_2 (Figure S3). This material is available free of charge via the Internet at http://pubs.acs.org.

References and Notes

(1) Berthelot, M.; Hebd, C. R. *Seances Acad. Sci.* **1866**, *62*, 905.
(2) Badger, G. M.; Lewis, G. E.; Napier, I. M. *J. Chem. Soc.* **1960**, 2825.
(3) Benson, S. W. *Thermochemical Kinetics*; Wiley-Interscience: New York, 1968.
(4) Reppe, W.; Schweckendiek, W. J. *Justus Liebigs Ann. Chem.* **1948**, *560*, 104.
(5) Grothahn, D. B. Transition Metal Alkyne Complexes: Transition Metal-Catalyzed Cyclotrimerization. In *Comprehensive Organometallic Chemistry II*; Abel, E. W., Stone, F. G. A., Wilkinson, G., Eds.; Hegedus, L. S., Vol. Ed.; Pergamon: Oxford, U.K., 1995; Vol. 12, p 741.
(6) Schore, N. E. *Chem. Rev.* **1988**, *88*, 1081.
(7) Saito, S.; Yamamoto, Y. *Chem. Rev.* **2000**, *100*, 2901.
(8) Gandon, V.; Aubert, C.; Malacria, M. *Chem. Commun.* **2006**, 2209.
(9) Chopade, P. R.; Louie, J. *Adv. Synth. Catal.* **2006**, *348*, 2307.
(10) Judai, K.; Wörz, A. S.; Abbet, S.; Antonietti, J. M.; Heiz, U.; Vitto, A. D.; Giordano, L.; Pacchioni, G. *Phys. Chem. Chem. Phys.* **2005**, *7*, 955.
(11) Boudjahem, A. G.; Monteverdi, S.; Mercy, M.; Bettahar, M. M. *Appl. Catal., A* **2003**, *250*, 49.
(12) Judai, K.; Abbet, S.; Wörz, A. S.; Ferrari, A. M.; Giordano, L.; Pacchioni, G.; Heiz, U. *J. Mol. Catal. A: Chem.* **2003**, *199*, 103.
(13) Boonstra, A. H.; Mutsaers, C. A. H. A. *J. Phys. Chem.* **1975**, *79*, 2025.
(14) Enerson, T. B.; Haas, H.; Zarrabi, K.; Titus, R. L. *Radiocarbon* **1998**, *40*, 167.
(15) Ma, Z.; Zaera, F. *Surf. Sci. Rep.* **2006**, *61*, 229.
(16) Abdelrehim, I. M.; Thornburg, N. A.; Sloan, J. T.; Caldwell, T. E.; Land, D. P. *J. Am. Chem. Soc.* **1995**, *117*, 9509.
(17) Kyriakou, G.; Kim, J.; Tikhov, M. S.; Macleod, N.; Lambert, R. M. *J. Phys. Chem. B* **2005**, *109*, 10952.
(18) Abdelrehim, I. M.; Pelhos, K.; Madey, T. E.; Eng, J., Jr.; Chen, J. G. *J. Mol. Catal. A: Chem.* **1998**, *131*, 107.
(19) Xu, C.; Peck, J. W.; Koel, B. E. *J. Am. Chem. Soc.* **1993**, *115*, 751.
(20) Pierce, K. G.; Barteau, M. A. *J. Phys. Chem.* **1994**, *98*, 3882.
(21) Diebold, U. *Surf. Sci. Rep.* **2003**, *48*, 53.
(22) (a) Abbet, S.; Sanchez, A.; Heiz, U.; Schneider, W. D.; Ferrari, A. M.; Pacchioni, G.; Rösch, N. *J. Am. Chem. Soc.* **2000**, *122*, 3453. (b) Ferrari, A. M.; Giordano, L.; Rösch, N.; Heiz, U.; Abbet, S.; Sanchez, A.; Pacchioni, G. *J. Phys. Chem. B* **2000**, *104*, 10612. (c) Cinquini, F.; Valentin, C. D.; Finazzi, E.; Giordano. L.; Pacchioni, G. *Theor. Chem. Acc.* **2007**, *117*, 827.
(23) Gilb, S.; Arenz, M.; Heiz, U. *Low Temp. Phys.* **2006**, *32*, 1097.
(24) Kirchner, K.; Calhorda, M. J.; Schmid, R.; Veiros, L. F. *J. Am. Chem. Soc.* **2003**, *125*, 11721.
(25) Pacchioni, G.; Lambert, R. M. *Surf. Sci.* **1994**, *304*, 208.
(26) Ferrari, A. M.; Giordano, L.; Pacchioni, G.; Abbet, S.; Heiz, U. *J. Phys. Chem. B* **2002**, *106*, 3173.
(27) Chrétien, S.; Salahub, D. *J. Chem. Phys.* **2003**, *119*, 12291.
(28) Momoh, P. O.; Abrash, S. A.; Mabrouki, R.; El-Shall, M. S. *J. Am. Chem. Soc.* **2006**, *128*, 12408.
(29) Momoh, P. O.; El-Shall, M. S. *Chem. Phys. Lett.* **2007**, *436*, 25.
(30) Martinez, M.; Michelini, M. C.; Rivalta, I.; Russo, N.; Sicilia, E. *Inorg. Chem.* **2005**, *44*, 9807.
(31) Zhou, M. F.; Andrews, L. *J. Phys. Chem. A* **1999**, *103*, 2066.
(32) Jackson, T. C.; Carlin, T. J.; Freiser, B. S. *J. Am. Chem. Soc.* **1986**, *108*, 1120.
(33) Buckner, S. W.; MacMahon, T. J.; Byrd, G. D.; Freiser, B. S. *Inorg. Chem.* **1989**, *28*, 3511.
(34) Knickelbein, M. B. *Annu. Rev. Phys. Chem.* **1999**, *50*, 79.
(35) He, S. G.; Xie, Y.; Dong, F.; Bernstein, E. R. *J. Chem. Phys.* **2006**, *125*, 164306.
(36) Braunstein, P.; Matt, D.; Nobel, D. *Chem. Rev.* **1988**, *88*, 747.
(37) Jiang, L.; Xu, Q. *J. Phys. Chem. A* **2007**, *111*, 3519.
(38) Weckhuysen, B. M.; Keller, D. E. *Catal. Today* **2003**, *78*, 25.
(39) Fierro, J. L. G. *Metal Oxides*; Taylor & Francis Group, LLC: London, **2006**.
(40) Dong, F.; Heinbuch, S.; Xie, Y.; Rocca, J. J.; Bernstein, E. R.; Wang, Z. C.; Deng, K.; He, S.-G. *J. Am. Chem. Soc.* **2008**, *130*, 1932.
(41) Frisch, M. J.; Trucks, G. W.; Schlegel, H. B.; Scuseria, G. E.; Robb, M. A.; Cheeseman, J. R.; Montgomery, J. A., Jr.; Vreven, T.; Kudin, K. N.; Burant, J. C.; Millam, J. M.; Iyengar, S. S.; Tomasi, J.; Barone, V.; Mennucci, B.; Cossi, M.; Scalmani, G.; Rega, N.; Petersson, G. A.; Nakatsuji, H.; Hada, M.; Ehara, M.; Toyota, K.; Fukuda, R.; Hasegawa, J.; Ishida, M.; Nakajima, T.; Honda, Y.; Kitao, O.; Nakai, H.; Klene, M.; Li, X.; Knox, J. E.; Hratchian, H. P.; Cross, J. B.; Bakken, V.; Adamo, C.; Jaramillo, J.; Gomperts, R.; Stratmann, R. E.; Yazyev, O.; Austin, A. J.; Cammi, R.; Pomelli, C.; Ochterski, J. W.; Ayala, P. Y.; Morokuma, K.; Voth, G. A.; Salvador, P.; Dannenberg, J. J.; Zakrzewski, V. G.; Dapprich, S.; Daniels, A. D.; Strain, M. C.; Farkas, O.; Malick, D. K.; Rabuck, A. D.; Raghavachari, K.; Foresman, J. B.; Ortiz, J. V.; Cui, Q.; Baboul, A. G.; Clifford, S.; Cioslowski, J.; Stefanov, B. B.; Liu, G.; Liashenko, A.; Piskorz, P.; Komaromi, I.; Martin, R. L.; Fox, D. J.; Keith, T.; Al-Laham, M. A.; Peng, C. Y.; Nanayakkara, A.; Challacombe, M.; Gill, P. M. W.; Johnson, B.; Chen, W.; Wong, M. W.; Gonzalez, C.; Pople, J. A. *Gaussian 03*, revision C.02; Gaussian, Inc.: Wallingford, CT, 2004.
(42) Schlegel, H. B. *J. Comput. Chem.* **1982**, *3*, 214.
(43) Peng, C.; Schlegel, H. B. *Isr. J. Chem.* **1994**, *33*, 449.
(44) Peng, C.; Ayala, P. Y.; Schlegel, H. B.; Frisch, M. J. *J. Comput. Chem.* **1996**, *17*, 49.
(45) Gonzalez, C.; Schlegel, H. B. *J. Chem. Phys.* **1989**, *90*, 2154.
(46) Gonzalez, C.; Schlegel, H. B. *J. Phys. Chem.* **1990**, *94*, 5523.
(47) Becke, A. D. *Phys. Rev. A* **1988**, *38*, 3098.
(48) Becke, A. D. *J. Chem. Phys.* **1993**, *98*, 5648.
(49) Lee, C.; Yang, W.; Parr, R. G. *Phys. Rev. B* **1988**, *37*, 785.
(50) Schafer, A.; Huber, C.; Ahlrichs, R. *J. Chem. Phys.* **1994**, *100*, 5829.
(51) Boys, S. F.; Bernardi, F. *Mol. Phys.* **1970**, *19*, 553.
(52) Pedley, J. B.; Marshall, E. M. *J. Phys. Chem. Ref. Data* **1983**, *12*, 967.
(53) Hildenbrand, D. L. *Chem. Phys. Lett.* **1976**, *44*, 281.
(54) Balducci, G.; Gigli, G.; Guido, M. *J. Chem. Phys.* **1983**, *79*, 5616.
(55) Cocke, D. L.; Gingerich, K. A. *J. Chem. Phys.* **1972**, *57*, 3654.
(56) Gupta, S. K.; Gingerich, K. A. *J. Chem. Phys.* **1981**, *74*, 3584.
(57) Cox, J. D.; Wagman, D. D.; Medvedev, V. A. *Codata Key Values for Thermodynamics*; Hemisphere Publishing Corp.: New York, 1984; p 1.
(58) Prosen, E. J.; Gilmont, R.; Rossini, F. D. *J. Res. Natl. Bur. Stand. (U.S.)* **1945**, *34*, 65.
(59) Schröder, D.; Shaik, S.; Schwarz, H. *Acc. Chem. Res.* **2000**, *33*, 139.
(60) Reed, A. E.; Curtiss, L. A.; Weinhold, F. *Chem. Rev.* **1988**, *8*, 899 and related references therein.
(61) Miao, L.; Dong, J.; Yu, L.; Zhou, M. F. *J. Phys. Chem. A* **2003**, *107*, 1935.
(62) Wang, G. J.; Chen, M. H.; Zhao, Y. Y.; Zhou, M. F. *Chem. Phys.* **2006**, *322*, 354.
(63) O' Hair, R. A. J.; Khairallah, G. N. *J. Cluster Sci.* **2004**, *15*, 331.
(64) Bohme, D. K.; Schwarz, H. *Angew. Chem., Int. Ed.* **2005**, *44*, 2336.
(65) O'Hair, R. A. J. *Chem. Commun.* **2006**, 1469.